

effect of spurious fluctuation of the cold start in the water level time series, the simulation result which lies within the first week of both runs was not used in quantitative measuring of skill assessment criteria.

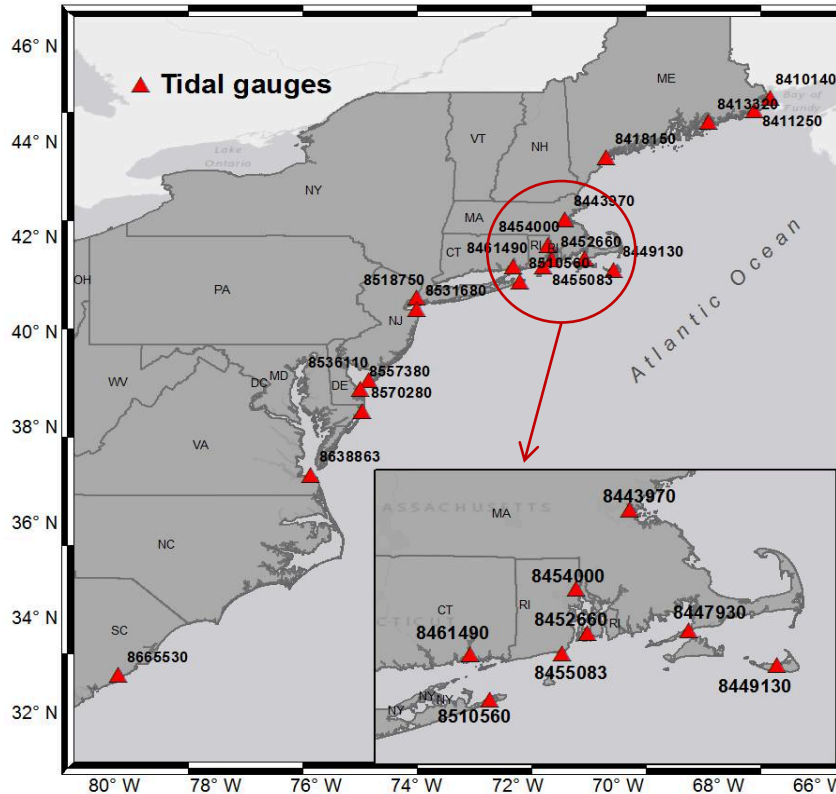


Figure 2. Schematic layout of the U.S. Northeast Mid-Atlantic Coast. The Red small triangles are observational measuring gauges which operates by NOAA.

MODEL SKILL METRICS

Comparison of model and observations

The most conventional way to compare simulated model variables with measurements is visual comparison. However, with advancement in measurement technologies, a dense observational data set is available to be used in model validation or skill assessment. Thus, it is necessary to provide objective means to quantitatively assess the quality of the model's performance. Therefore, a set of statistical measures and procedures are needed to conduct a comprehensive analysis of differences between model and measurement data in a way that is suitable to a specific application.

There are a number of statistical measures that are useful to assess the model's behavior. There is no consensus on which statistical metric is the best in revealing the quality of a model's performance. Therefore, it is useful to employ several statistical tests to quantify misfit among the same set of data. Thus, the model's performance should be evaluated using several metrics. (Stow et al. 2009).

Criteria Definition

In this study, number of statistical indices such Normalized Root-Mean Square Deviation (NRMSD), Coefficient of Determination (R^2), Scatter Index (SI), and Normalized Bias (NB) are used to quantify the misfit between model simulated variables and corresponding observation

data; Denoting N = number of observations, a set of model simulation values as m , a set of observation values or known values as O , overbar is mean of the set. They are defined as:

$$\text{NRMSD} = \sqrt{\frac{\frac{1}{N} \sum_{i=1}^N (O_i - m_i)^2}{\text{Max}(O_i)}} \quad (1)$$

The NRMSD in Eq. (1) is a frequently-used measure for discrepancies between the model prediction and the values actually observed. The maximum value of the observation set was chosen to normalize the root-mean square deviation. This index can indicate the model prediction accuracy in reproducing observation.

$$R^2 = 1 - \frac{SS_{\text{res}}}{SS_{\text{tot}}} \quad (2)$$

In Coefficient of Determination (R^2) where variance of observation data is $SS_{\text{tot}} = \sum_i (O_i - \bar{O})^2$, the sum of residual square $SS_{\text{res}} = \sum_i (O_i - m_i)^2$, and average of observation values $\bar{O} = \frac{1}{N} \sum_{i=1}^N O_i$. Coefficient of determination, which is the square of the correlation coefficient, is a measure of the goodness-of-fit between the two time series. On the other hand, the more data on the regression line, the higher value of R^2 . If the prediction varies together with the observed data, a value near 1 (or 100%) can be achieved.

$$\text{NB} = \frac{\frac{1}{N} \sum_{i=1}^N E_i}{\frac{1}{N} \sum_{i=1}^N |O_i|} \quad (3)$$

where $E_i = m_i - O_i$ denotes the error between the modeled time series and measured data.

$$\text{SI} = \frac{\sqrt{\frac{1}{N} \sum_{i=1}^N (E_i - \bar{E})^2}}{\frac{1}{N} \sum_{i=1}^N |O_i|} \quad (4)$$

Where the average error is $\bar{E} = (1/N) \sum_{i=1}^N |O_i - m_i|$. The Scatter Index (SI) is the ratio of the standard deviation of the observation-to-prediction discrepancies to the average observation values (Hanson et al. 2009).

RESULT AND ANALYSIS

Comparing time series of tidal levels with observation (in time domain)

In this paper, the simulation result was compared with the observation data collected from the measurements collected at 19 stations over U.S. Northeast and Mid-Atlantic coast. In Figure 3, a visual comparison between the NOAA observed and modeled water level time series is displayed for number of stations. The figures start date is from 0:00 UTC July 30, 1991 to 0:00 UTC Aug 9, 1991. As the comparison shows, there is obvious spurious oscillation of water level at 12:00 UTC Aug 1, 1991 where the short simulation run began (green line).

This unrealistic water surface variation originates from a cold start run. Therefore, the first 7 days of both short and long simulation run were removed from the skill assessment metric's measurements.

There is a good agreement between model result and observation data set observed in visual illustration. However, there are some misfits between the observed and modeled water level.

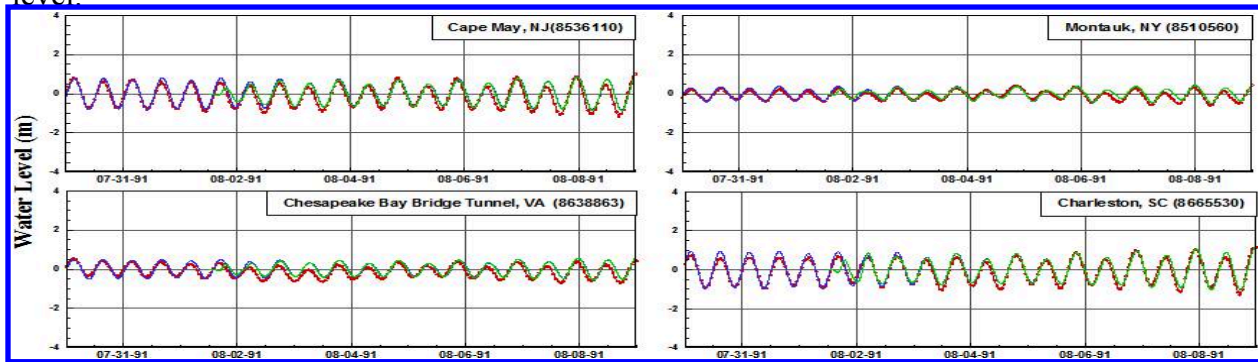


Figure 3. Water level Time series at number of NOAA gauge stations. Observed values are shown in red line with red circles attached to it; modeled time series are shown in blue color and line in green color is for the long and short simulation run, respectively.

Comparing tidal constituents with known values (provided by NOAA)

Tidal harmonic constituents were derived from the time series using harmonic analysis procedure. Newly-developed parameter identification was used to identify harmonic constants using modeled time series under astronomical tide simulation only. Skill assessment criteria were computed based on the identified amplitudes and phases at several stations. The modeled time series, obtained from long run simulation (108 days), is used for the harmonic analysis procedure.

The optimization procedure performed better using modeled time series from the long run simulation than from the short run. This is why identified parameters, which harmonically analyzed from the long run simulation, are presented. In this part, the Normalized Root-Mean-Square Deviation (NRMSD) criteria were used to measure how well the optimization was performed.

Analysis of assessment results in time domain

All three statistical indices employed as metric are shown in Figure 4. The values of computed indices are in a very good range which indicates the model performed well in reproducing water surface elevation across the computational domain. For instance, the large values of R^2 indicate that good accuracy in replicating flow circulation was achieved. On the other hand, the regression line passes nearly through 90% and greater of the points on a scatter plot. The highest linearity between the observation and simulation exists in East port and Cape May with 96%, while R^2 at Charleston is the lowest.

The Average Bias value illustrates that the model overestimates in reproducing water level time series. At Charleston, Averaged Bias and Scatter Index (SI) are relatively large. This may be attributed to many factors such as the location of NOAA water level measuring gauges which may possibly be located in the bay or behind a barrier in embayment. Thus, it makes the model unable to capture well the flow circulation around them.

Similarly, relatively large Averaged Bias in Chesapeake Bay Bridge, Lewese, the Battery, Newport, and Boston can arise from poor mesh in computational domain near these stations. Near these stations, a finer mesh is required to capture small variabilities that affect modeled time series.

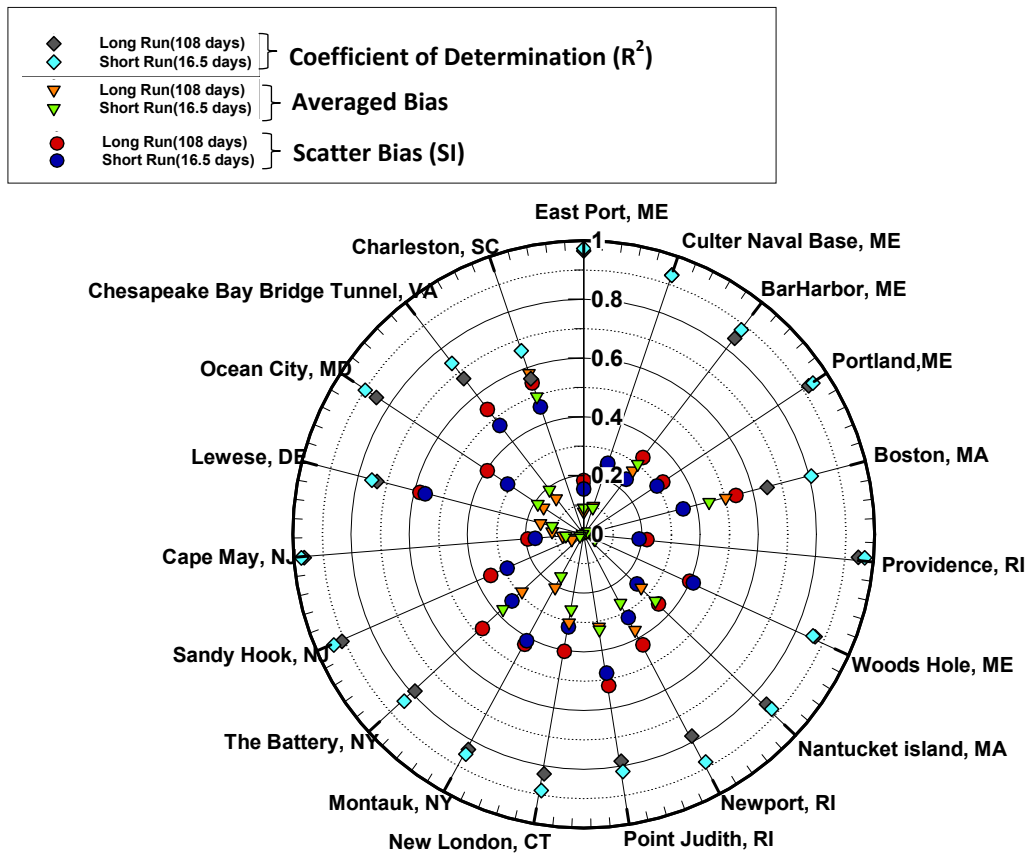


Figure 4. Computed values of three criteria used in this paper which are illustrated in a radar plot; Coefficient of Determination (Diamond), Averaged Bias (Gradient), and Scatter Index (Circle).

Analysis of assessment results of identified constituents

The tide harmonic constituents obtained from the parameter identification were compared to known values. The statistical index, NRMSD, were computed to measure the model skill with respect to the seven main tidal harmonic constituents; semi-diurnal constants, including M2, S2, N2, and K2 as well as O1, Q1, and K1 as diurnal tide components. The result suggests that, regardless of physical geographic location and accuracy of reproduced time series, the parameter identification approach performed much better in identifying amplitude (red) than phase (blue) (Figure 5).

The result indicated that the identification accuracy in identifying semi-diurnal tide constituents is greater than diurnal tide components (Figure 5). This can be attributed to the stronger semi-diurnal tide signals as well as the larger range of semi-diurnal amplitude in the Atlantic Ocean. Accuracy of identified phase with regard to known values is slightly different from accuracy which obtained in identified amplitudes (Figure 5).

The average value of NRMSD in identified phases is 31%. As mentioned earlier, the accuracy of identified harmonic constituents depends not only on modeled time series. Strength of parameter identification in identifying parameters is also dependent on many factors which will be explained in the next sections.

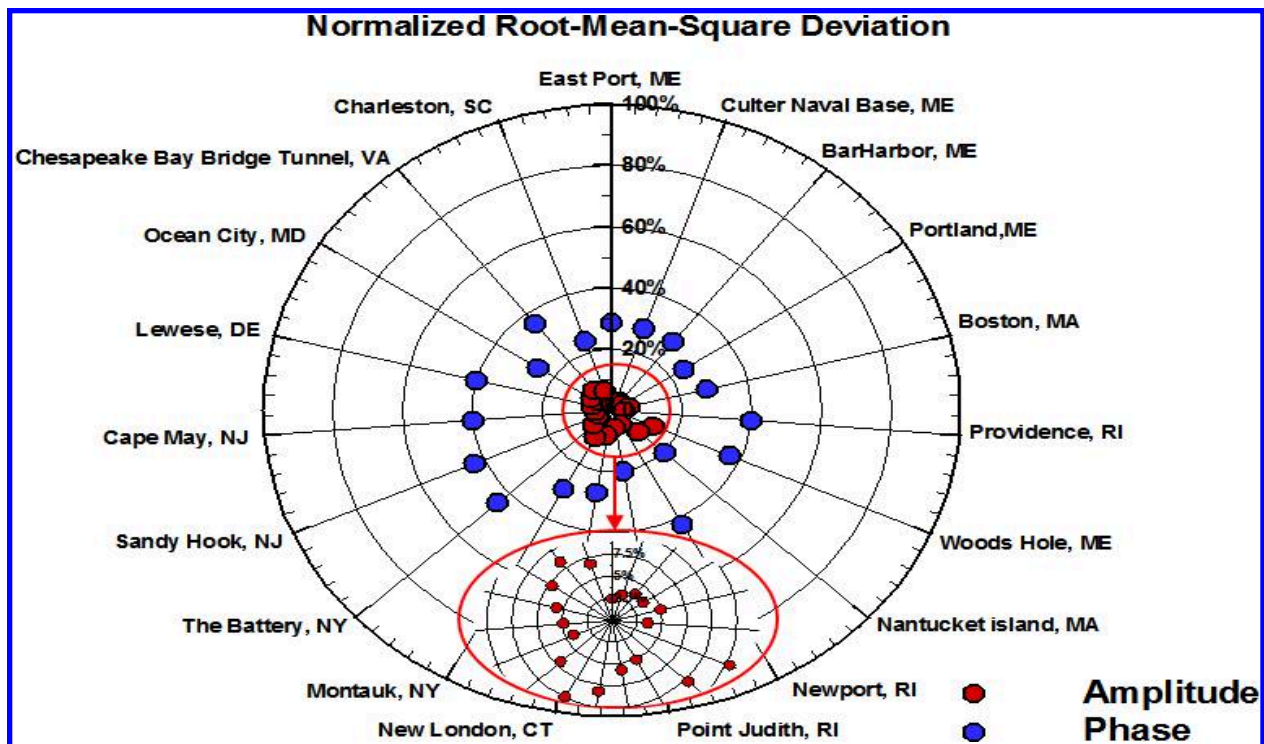


Figure 5. Skill assessment metric, Normalized Root-Mean-Square Deviation in identifying Amplitude.

Harmonic Analysis

The routine prediction of tides at selected coastal stations is based on a simple principle. This principle asserts that for any linear system whose forces can be decomposed into a sum of harmonics having the same frequencies but with different amplitudes and phases from the forces. Water elevation variation, for the tidal decomposition, can be written as:

$$X(t) = X_0 + \sum_1^N f_i A_i \cos(\omega_i t + V_i + u_i - \psi_i) \quad (5)$$

Where N is number of tidal components, X_0 is initial water level, A_i is constant amplitudes, and ψ_i is constant phase (epochs). Nodal factor is given by f_i and the equilibrium argument by $V_i + u_i$. Among these terms, only the frequencies are an absolute constant for given constituents (Herbich 1999).

Parameter Identification Procedures

An efficient method of parameter identification is to take advantage of optimal control theories to minimize overall discrepancies between water level time series (computed by traditional harmonic tide equation (Equation 5)) and in-situ measurements collected from NOAA tide and current website. The discrepancies can be generally defined as a performance function in the form of:

$$J(X) = \sum_{j=1}^M (X_j^{cal} - X_j^{obs})^2 \quad (6)$$

Where J is performance function that computes square error between water level computed by harmonic tide equation (Equation 5) and observation data collected at each NOAA station. An iterative procedure is employed to minimize the performance function.

The L-BFGS algorithm is capable of optimizing unconstrained problems, executed in parameter identification procedure (Ding et al. 2004). In L-BFGS algorithm, the norm of gradient of the objective function, with regard to the two parameters were calculated, was computed (at each iteration) in order to check if the optimal solution had been reached. Gradients of performance function with regard to amplitude and phase are presented in Equation 7 and 8.

$$\frac{\partial J}{\partial A_i} = 2 \sum_{j=1}^M (X_j^{cal} - X_j^{obs}) \sum_1^N f_i \cos(\omega_i t + V_i + u_i - \psi_i) \quad (7)$$

$$\frac{\partial J}{\partial \psi_i} = 2 \sum_{j=1}^M (X_j^{cal} - X_j^{obs}) \sum_1^N f_i A_i \sin(\omega_i t + V_i + u_i - \psi_i) \quad (8)$$

SUMMARY AND CONCLUSION

In this study, an integrated coast-ocean circulation model, CCHE2D-Coast, was validated. The model performance was evaluated and the errors associated with modeled water level time series were quantified through two approaches. In the first approach, the misfit between time-dependent water surface elevation and observed data was quantified at several NOAA monitoring tidal gauges. As a second approach, harmonic analysis was performed to identify the tidal constituent parameters. Then, the discrepancies between identified tidal harmonic components and known values were computed.

In this study, a suite of metrics comprised of Normalized Root-Mean Square Deviation, Coefficient of Determination, Scatter Index, and Averaged Bias is used to quantitatively assess the model performance in reproducing flow circulation. Overall, the extent to which most metrics were obtained suggests that there is good agreement between the modeled time series and observed data in the majority of monitoring points. Therefore, it is ascertained that the set of time series used in the harmonic analysis have good accuracy.

To determine the tidal harmonic components, amplitude and phase, a newly-developed parameter identification approach was used to identify harmonic constituents. A phase shift may exist in modeled time series, which can cause an incorrect comparison between set of data points. Therefore, comparing tidal harmonic components can eliminate some sources of errors that stem from a possible phase-lag between observation and model-simulated results. The identified tidal constituent parameters, amplitudes and phases, are used to compute the employed criterion with respect to the known values. The result of statistical analysis revealed that the accuracy in identifying amplitudes is higher than in identifying phases.

The results demonstrated that the model, driven by astronomical tide-only forces, was able to accurately capture ocean-coast flow dynamics across the U.S. East Coast where complex geometry exists. To further enhance the model skill in simulation of the tide currents, a finer resolution within computational domain must be taken in shallow water regions. In addition, taking into account some other forces such as pressure and winds can improve the accuracy of the simulation result.

REFERENCE

- Pain, C.C, Piggott, M.D., Goddard, A.J.H, Fang, F., Gorman, G.J., Marshall, D.P., Eaton, M., Power, P.W., de Oliveira, C.R.E. (2005). Three-dimensional unstructured mesh ocean modelling, *Ocean Modell*, 10 pp. 5–33.
- Chen, C., Liu, H., Beardsley, R. C. (2003). An unstructured grid, finite-volume, three-dimensional, primitive equations ocean model: Applications to coastal ocean and estuaries. *J. Atmos. Ocean. Tech.* 20, 159-186.

- Lynch, D., McGillicuddy, D., Werner, F. (2009). Skill Assessment for Coupled Physical-Biological Models of Marine Systems, special issue of *J. Marine Systems*, 250pp.
- Ding, Y., Jia Y., and Wang, S. S. Y. (2004). Identification of the Manning's roughness coefficients in shallow water flows, *Journal of Hydraulic Engineering*, ASCE, Vol. 130, No.6, pp.501-510.
- Ding, Y., Wang, S. S. Y., and Jia, Y. (2006). Development and validation of a quasi-three-dimensional coastal area morphological model, *J. Waterway, Port, Coastal, and Ocean Engineering*, ASCE, Vol.132, No.6, pp. 462-476.
- Ding, Y. and Wang, S. (2008). Development and Application of a Coastal and Estuarine Morphological Process Modeling System. *Journal of Coastal research*, pp. 127-140.
- Ding, Y., Zhang, Y.-X., and Jia, Y. (2013). Graphical User Interface for CCHE2DCoast – Quick Start Guide, August, 2013.
- Ding, Y., Zhang, Y., Jia, Y., Gazerzadeh, A., Altinakar, M.S. (2014). Simulation and Prediction of Storm Surges and Waves Driven by Hurricanes and Assessment of Coastal Flooding and Inundation. ICHE, Hamburg.
- Gazerzadeh, A., Ding, Y., Zhang, Y., Jia, Y., Altinakar, M.S. (2015). Hindcasting Storm Surge and Waves in Hurricane Bob in the Gulf of Maine Using CCHE2D-Coast. *World Environmental and Water Resources Congress 2015*: pp. 1512-1521.doi: 10.1061/9780784479162.148
- Hanson, J. L., B. A. Tracy, H. L. Tolman, and R. D. Scott, (2009). Pacific hindcast performance of three numerical wave models .*J. Atmos. Oceanic Technol.*, 26, 1614–1633.
- Herbich, J. B. (1999) *Handbook of coastal engineering*, McGraw-Hill.
- Jia, Y., Wang, S. and Xu, Y. (2002). Validation and Application of a 2D model to Channel with Complex Geometry. *Int.J. Comput, Engineering Science*, pp. 3(1), 57-71.
- Liu, D. C., and Nocedal, J. (1989). On the limited memory method for large scale optimization.” *Math. Program*, 45-3, 503–528.
- Luettich, R., Westerink, J. J., Scheffner, N.W. (1992). ADCIRC: an advanced three-dimensional circulation model for shelves coasts and estuaries, report 1: theory and methodology of ADCIRC-2DDI and ADCIRC-3DL. *Dredging Research Program Technical Report DRP-92-6*, U.S. Army Engineers Waterways Experiment Station, Vicksburg, MS, page 137.
- Mukai, A.Y., Westerink, J. J., and Luettich, R. A. (2001). Guidelines for using Eastcoast 2001 database of tidal constituents within Western North Atlantic Ocean, Gulf of Mexico and Caribbean, *Coastal and Hydraulics Engineering Technical Note CHETN-IV-40*, U.S. Army Engineer Research and Development Center, Vicksburg, MS. <http://chl.wes.army.mil/library/publications/chetn/>
- Piggott, M. D., Pain, C. C., Gorman, G. J., Marshall, D. P., Killworth, P. D. (2008). Unstructured adaptive meshes for ocean modeling. In: *Ocean modeling in an eddying regime*, Ed. M. W. Hecht and H. Hasumi, *Geophysical Monograph 177*, AGU, 383-408.
- Stow, C.A., Joliff, J., McGillicuddy, D.J., Doney, S.C., Allen, J.I., Friedrichs, M.A.M., Rose, K.A., Wallhead, P. (2009). Skill assessment for coupled biological/physical models of marine systems. *Journal of Marine Systems* 76 (1e2).
- Westerink, J. J., and Gray, W. G. (1991). Progress in surface water modeling. *Reviews in Geophysics*, 29, 210–217.

Three-Dimensional Numerical Modeling of the Temperature Distribution in a High Dam Reservoir on the Mekong River

Xiaobo Chao¹; Yun Deng²; and Yafei Jia³

¹National Center for Computational Hydroscience and Engineering, Univ. of Mississippi, 332 Brevard Hall, University, MS 38677. E-mail: chao@ncche.olemiss.edu

²State Key Laboratory of Hydraulics and Mountain River Engineering, Sichuan Univ., Chengdu 610065, China. E-mail: dengyun@scu.edu.cn

³National Center for Computational Hydroscience and Engineering, Univ. of Mississippi, 328 Brevard Hall, University, MS 38677. E-mail: jia@ncche.olemiss.edu

Abstract

Xiaowan Reservoir was created by the construction of Xiaowan Dam on Mekong River. This dam is the second highest arch dam in the world with 292 m tall and 902 m long. The reservoir is about 178km from upstream to the dam, and the surface area is around 189 km². The water depth near the dam is very deep, which normally varies from 200 to 270m seasonally. For such a deep reservoir, the vertical temperature distribution show a significant stratified structure. In this study, a three dimensional numerical model was developed for simulating the flow fields and temperature distribution in Xiaowan reservoir near the dam. The effects of buoyancy on the momentum equations and turbulence transport equations was considered. For turbulence closure, the buoyancy-extended version of k-ε model was used. The model was first validated using a laboratory case of turbulent buoyant flow in a curved open channel, and then it was applied to simulate the flow and temperature in Xiaowan Reservoir. The numerical results were compared with field measurements, and the physical characteristics of flow pattern and temperature distribution in the reservoir were discussed.

INTRODUCTION

Many dams have been built with the intention to improve human quality of life by diverting water for hydroelectric power, irrigation, drinking water supply, navigation, and flood control. The dammed reservoirs benefit people by providing usable and reliable water sources. However, adverse environmental impacts have been identified during and after many dammed reservoir constructions. It may greatly affect the river hydrology, sedimentation, temperature distribution, and aquatic ecosystems.

Mekong River is the 7th longest river in Asia, and the 12th longest in the world. It has a length of about 4,350 km. Rising in southeastern Qinghai province, China, it flows through the eastern part of the Tibet Autonomous Region and Yunnan province, after which it forms part of the international border between Myanmar (Burma) and Laos, as well as between Laos and

Thailand. The river then flows through Laos, Cambodia, and Vietnam before draining into the South China Sea (Fig. 1). It plays an important role in the economic development of these six countries. Currently, 8 dams have been constructed or under construction on the upper Mekong River in China, and 12 dams have been planned or under construction on the lower Mekong River in other countries (Fig. 1). Mekong River is an international river, and the constructions of dams on the river have become a major environmental concern of these countries.

Xiaowan dam, one of eight dams on the upper Mekong River in China, was constructed between 2002 and 2010. It is a 292 m tall and 902 m long double-curvature arch dam, the second highest arch dam in the world. The water depth near the dam is very deep, which normally varies from 200 to 270m seasonally. Heihui River flows into Mekong River from left bank at about 1.5 km upstream of the dam. Its yearly averaged discharge is only 5% of Mekong River. Mekong River contributes major flow discharge to the reservoir. Figure 2 shows the dammed reservoir. The water intake of the power station is located on the right bank of the river. The climate in Xiaowan Reservoir belongs to the typical subtropical low latitude mountain monsoon climate (Xu et al 2014). Due to the deep water depth near the dam, a strong temperature stratification is formed generally between March and November. The curvature of Mekong River may also affect the temperature distribution in the reservoir.



Figure 1. Dams on Mekong River
(from www.meltdownintibet.com)

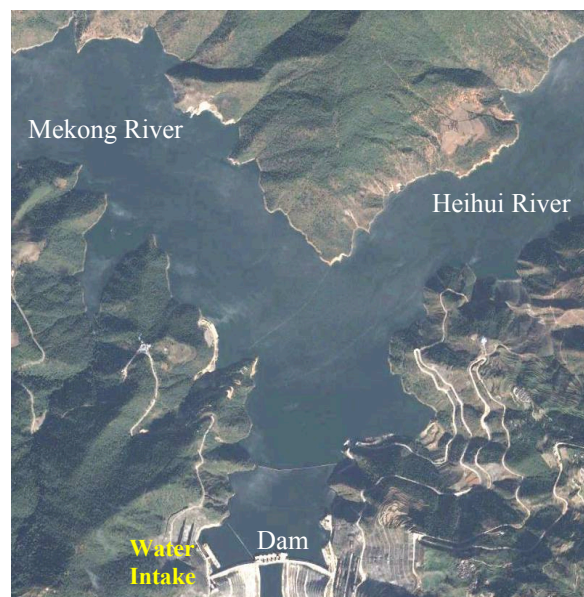


Figure 2. Xiaowan Dammed Reservoir

A 3D numerical model was developed to simulate the turbulence flow and temperature distribution based on CCHE3D model (Jia, et al 2005) by considering the buoyancy influences. The heat exchanges between atmosphere and water surface due to solar radiation, long-wave radiation, evaporation, conduction and convection were considered as source terms in the model. Experimental results of turbulent buoyant flow in a curved open channel were used to test model. The model was applied to simulate the flow and temperature distribution in Xiaowan reservoir. The field measured data was used to calibrate the model. The simulated vertical temperature distributions were generally in good agreement with field observations. Both model results and

field observations show the temperature at the outlet of the dam is around 14-16°C in February and 15-17°C in May. The simulated results provide useful information to understand the temperature distribution in high dam reservoir and analyze the effect of high dam reservoir on the downstream water temperature.

MODEL DESCRIPTION

To simulate the flow and temperature distribution in a high dam reservoir, a numerical model was developed based on CCHE3D hydrodynamic model (Jia et al. 2005). CCHE3D is a finite-element-based unsteady 3D turbulence model that can be used to simulate turbulent flows with irregular boundaries and free surfaces. This model is based on the 3D Reynolds-averaged Navier-Stokes equations. By applying the Boussinesq assumption, the turbulent stresses are approximated by the eddy viscosity and the strains of the flow. There are several turbulence closure schemes available including: parabolic eddy viscosity model, mixing length model, k-ε model and nonlinear k-ε model. This model has been verified against analytical methods and experimental data representing a range of hydrodynamics phenomena.

In the proposed model, the heat transport equation was solved using a finite element method consistent with the CCHE3D model. The influence of temperature on the flow density, momentum equations and k-ε equations were considered. The velocity and temperature fields were solved simultaneously.

Governing Equations for Turbulence Flow

Using the Boussinesq approximation for small density differences, the governing equation of momentum of three-dimensional unsteady hydrodynamic model can be written as follows:

$$\frac{\partial u_i}{\partial t} + u_j \frac{\partial u_i}{\partial x_j} = -\frac{1}{\rho_r} \frac{\partial p}{\partial x_i} + \frac{\partial}{\partial x_j} \left(\nu \frac{\partial u_i}{\partial x_j} - \overline{u_i u_j} \right) + g_i \frac{\rho - \rho_r}{\rho_r} \quad (1)$$

The continuity equation can be written as

$$\frac{\partial u_i}{\partial x_i} = 0 \quad (2)$$

where u_i ($i=1,2,3$) = Reynolds-averaged flow velocities (u_x, u_y, u_z) in a Cartesian coordinate system (x,y,z); t = time; p = pressure; ν = fluid kinematic viscosity; $-\overline{u_i u_j}$ = Reynolds stress; g_i = acceleration due to gravity in the i^{th} direction; ρ_r = reference water density; ρ = density of thermal flow (kg/m^3), which may be calculated by (Shen et al. 2003):

$$\begin{aligned} \rho = & (0.102027692 \times 10^{-2} + 0.677737262 \times 10^{-7} T - 0.905345843 \times 10^{-8} T^2 \\ & + 0.864372185 \times 10^{-10} T^3 - 0.642266188 \times 10^{-12} T^4 + 0.105164434 \times 10^{-17} T^7 \\ & - 0.104868827 \times 10^{-19} T^8) \times 9.8 \times 10^5 \end{aligned} \quad (3)$$

where T = temperature ($^{\circ}\text{C}$). The free surface elevation (η) was computed using:

$$\frac{\partial \eta}{\partial t} + u_s \frac{\partial \eta}{\partial x} + v_s \frac{\partial \eta}{\partial y} - w_s = 0 \quad (4)$$